15 June 2001

ELSEVIER

Optics Communications 193 (2001) 161–173

OPTICS COMMUNICATIONS

www.elsevier.com/locate/optcom

Experimental verification of differences between classical and quantum polarization properties

Pavel Usachev [a,b], Jonas Söderholm [a,*], Gunnar Björk [a], Alexei Trifonov [a,b]

[a] *Department of Microelectronics and Information Technology, Royal Institute of Technology (KTH), Electrum 229, SE-164 40 Kista, Sweden*

[b] *Ioffe Physical Technical Institute, 26 Polytekhnicheskaya, 194021 St. Petersburg, Russia*

Received 20 November 2000; received in revised form 27 March 2001; accepted 3 April 2001

Abstract

We have carried out polarization measurements on a two-photon quantum state generated by spontaneous parametric down conversion. Our measurements show that the state is unpolarized in the classical theory, but they also show that the state is not invariant under geometric rotation. Therefore, it is not unpolarized in the quantum theory. This is another example of a rather simple experiment that clearly shows the effects of quantum interference. It also confirms the theoretical investigation by Klyshko [Phys. Lett. A 163 (1992) 349]. The experiment is explained theoretically and a systematic treatment of polarization in quantum theory is outlined. © 2001 Elsevier Science B.V. All rights reserved.

PACS: 42.50.−p; 42.50.Dv

Keywords: Quantum polarization; Stokes parameters; Stokes operators; Poincaré sphere; Photon pairs

1. Introduction

In the electromagnetic field theory, the linearly polarized modes of a monochromatic plane wave are easily understood, since the field can be decomposed into two waves with perpendicular oscillations. In classical optics, the polarization of such a plane wave is then unambiguously defined by the two components, and it is straightforward to construct elliptically and circularly polarized modes. The Stokes parameters, introduced in 1852 [1], offer a handy treatment of polarization properties in the classical theory [2]. The theory is easily extended to include stochastic (or quasi-monochromatic) waves [3,4], and one then naturally introduces the degree of polarization.

On the other hand, quantized fields may be entangled. This makes the notion of polarization much more complex in quantum theory. Earlier work on the quantum theory of polarization has focused on the Stokes operators [5]. It is, however, known that the Stokes operators cannot, in general, fully characterize a

* Corresponding author. Fax: +46-8-7521240.
E-mail address: jonas@ele.kth.se (J. Söderholm).

0030-4018/01/$ - see front matter
PII: S0030-4018(01)01252-4

quantum state [6–9]. The experiment reported here is an example of the failure of the Stokes-parameter point of view in quantum optics. Other examples where quantum interference gives very different results from classical interference are, of course, well known and have been shown experimentally (see Ref. [10] for a review). However, we think that the present example is particularly transparent, partly because it deals with the generally known concept of polarization. One aim of this paper is therefore to point out the effects of quantum interference to a broader audience, not only those already familiar with this kind of phenomena.

Furthermore, we demonstrate that the formalism used for the relative phase of two quantized modes [11–13] can be employed when considering quantum polarization properties. This offers a new way of tackling these problems, differing from the treatments by, for example, Klyshko [7] and Karassiov et al. [14].

The paper is organized as follows. In Section 2, a short introduction to the Stokes parameters and the Poincaré sphere is given. The corresponding Stokes operators used in quantum optics are introduced in Section 3. The classical theory of our experiment is described in Section 4, before the experimental details and results are reported in Section 5. It is found that our experiment cannot be explained by the classical theory, and consequently the fully quantum mechanical description of our experiment is given in Section 6. Our new formalism for quantum polarization is presented in Section 7. Finally, we summarize our paper in Section 8.

2. Stokes parameters and the Poincaré sphere

Let us denote the horizontal and vertical component of a classical electric field in a plane wave by E_1 and E_2, respectively. Recall that a geometric rotation of the field by θ about the propagation axis, as defined in Fig. 1, transforms its components according to

$$\begin{pmatrix} E_1' \\ E_2' \end{pmatrix} = \begin{pmatrix} \cos\theta & \sin\theta \\ -\sin\theta & \cos\theta \end{pmatrix} \begin{pmatrix} E_1 \\ E_2 \end{pmatrix}. \tag{1}$$

Similarly, if the vertical component is delayed by a phase shift ϕ, i.e., if the field propagates through a birefringent phase plate with its slow axis oriented in the vertical direction, we have

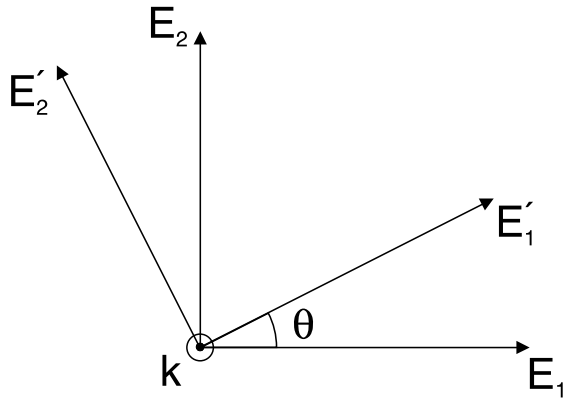

Fig. 1. Definition of the angle of geometric rotation θ. The arrows show the orientation of the modes, which are denoted by their components of the electric field. The arrows also define the respective positive field directions.

$$\begin{pmatrix} E_1' \\ E_2' \end{pmatrix} = \begin{pmatrix} 1 & 0 \\ 0 & \mathrm{e}^{-\mathrm{i}\phi} \end{pmatrix} \begin{pmatrix} E_1 \\ E_2 \end{pmatrix}. \tag{2}$$

Assume now that we have a monochromatic transverse field that is completely described by

$$E_1 = a_1 \mathrm{e}^{\mathrm{i}\varphi_1}, \quad E_2 = a_2 \mathrm{e}^{\mathrm{i}\varphi_2}, \qquad \varphi = \varphi_2 - \varphi_1, \tag{3}$$

where a_1, a_2, φ_1, φ_2, and hence φ are real. In classical optics, a usual way to treat polarization is by means of the Stokes parameters [3]. One of the four Stokes parameters is proportional to the intensity, and takes the form

$$S_0 = |E_1|^2 + |E_2|^2 = a_1^2 + a_2^2. \tag{4}$$

It is customary to normalize the other three Stokes parameters to this one according to

$$s_x = \frac{S_x}{S_0} = \frac{2\,\mathrm{Re}\{E_1^* E_2\}}{|E_1|^2 + |E_2|^2} = \frac{2a_1 a_2 \cos\varphi}{a_1^2 + a_2^2} = \sin\Theta \sin\Phi, \tag{5}$$

$$s_y = \frac{S_y}{S_0} = \frac{2\,\mathrm{Im}\{E_1^* E_2\}}{|E_1|^2 + |E_2|^2} = \frac{2a_1 a_2 \sin\varphi}{a_1^2 + a_2^2} = \cos\Theta, \tag{6}$$

$$s_z = \frac{S_z}{S_0} = \frac{|E_1|^2 - |E_2|^2}{|E_1|^2 + |E_2|^2} = \frac{a_1^2 - a_2^2}{a_1^2 + a_2^2} = \sin\Theta \cos\Phi. \tag{7}$$

Here Θ and Φ are the angles of the spherical coordinates for the point described by the Cartesian coordinates (s_x, s_y, s_z). One finds that the possible values of a_1, a_2, and φ ensure that the considered states are mapped on a sphere of unit radius, which in this context is called the Poincaré sphere. This mapping is one-to-one, i.e., for every polarization state there is a unique point on the sphere, and for every point there is a unique polarization state.

Fig. 2 shows the Poincaré sphere and the location of some different states of polarization. Note that, in order to use both the common nomenclature of quantum mechanics and the usual orientation of presentation of the Poincaré sphere, the orientation of the axes differs from the usual Cartesian system.

From Eq. (2) we see that phase-shifting component E_2 of the state (3) by ϕ relative to the component E_1 makes $a_1' = a_1$, $a_2' = a_2$, and $\varphi' = \varphi - \phi$. Thus, the Stokes parameters are transformed according to

$$\begin{pmatrix} s_x' \\ s_y' \\ s_z' \end{pmatrix} = \begin{pmatrix} \cos\phi & \sin\phi & 0 \\ -\sin\phi & \cos\phi & 0 \\ 0 & 0 & 1 \end{pmatrix} \begin{pmatrix} s_x \\ s_y \\ s_z \end{pmatrix}, \tag{8}$$

which describes a positive rotation around the s_z-axis by ϕ.

Similarly, if we apply a geometric rotation θ on the state (3), Eq. (1) tells us that

$$\begin{pmatrix} s_x' \\ s_y' \\ s_z' \end{pmatrix} = \begin{pmatrix} \cos 2\theta & 0 & \sin 2\theta \\ 0 & 1 & 0 \\ -\sin 2\theta & 0 & \cos 2\theta \end{pmatrix} \begin{pmatrix} s_x \\ s_y \\ s_z \end{pmatrix}. \tag{9}$$

Again, the transformation can be seen as a positive rotation, in this case by 2θ around the s_y-axis.

Suppose now that we measure the intensity of the horizontally polarized component. Since the intensity is proportional to the square of the electric field, we introduce

$$\begin{aligned} &I_1 = |E_1|^2 = a_1^2, \quad I_2 = |E_2|^2 = a_2^2, \\ &I_{\mathrm{tot}} = I_1 + I_2 = a_1^2 + a_2^2. \end{aligned} \tag{10}$$

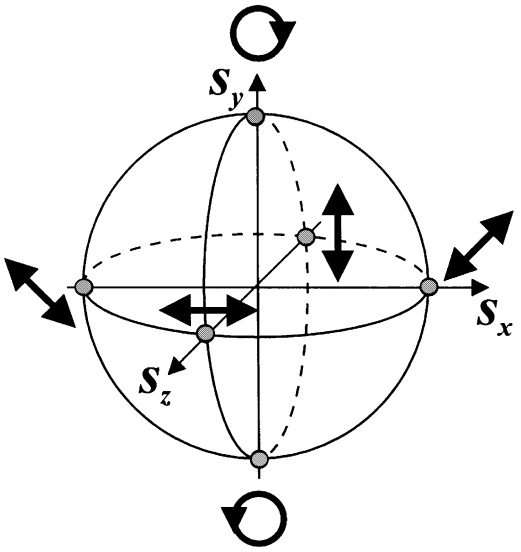

Fig. 2. All linearly polarized fields are found on the equator of the Poincaré sphere. The right- and left-hand circularly polarized fields are found on the north and south pole, respectively. Note that the orientation of the axes differs from the usual Cartesian system.

We note that

$$s_z = \frac{2a_1^2 - I_{\text{tot}}}{I_{\text{tot}}} \quad \Rightarrow \quad I_1 = a_1^2 = \frac{s_z + 1}{2} I_{\text{tot}}. \tag{11}$$

Thus, the normalized intensity of the horizontal mode can be read out from the Stokes parameter s_z.

3. Stokes operators

In quantum theory, the horizontal and vertical mode are characterized by their annihilation operators $\hat{a}$ and $\hat{b}$, respectively. By making use of the Heisenberg picture, the quantum states of the modes can be expressed in the annihilation operators. The transformations of these operators under geometric rotations and relative phase shifts are given by Eqs. (1) and (2), where E_1 and E_2 are replaced by $\hat{a}$ and $\hat{b}$, respectively.

In quantum optics, a set of operators are introduced [5,15–17] in correspondence to the Stokes parameters. The Stokes operators, which are of the same form as the angular momentum operators [18], are defined as

$$\widehat{S}_0 = \hat{a}^\dagger \hat{a} + \hat{b}^\dagger \hat{b}, \tag{12}$$

$$\widehat{S}_x = \hat{a}^\dagger \hat{b} + \hat{a}\hat{b}^\dagger, \tag{13}$$

$$\widehat{S}_y = \mathrm{i}(\hat{a}\hat{b}^\dagger - \hat{a}^\dagger \hat{b}), \tag{14}$$

$$\widehat{S}_z = \hat{a}^\dagger \hat{a} - \hat{b}^\dagger \hat{b}. \tag{15}$$

Again, we find that the operators are transformed by a geometric rotation or a relative phase shift in exactly the same manner as their classical counterparts. We simply replace s_x, s_y, and s_z with $\widehat{S}_x$, $\widehat{S}_y$, and $\widehat{S}_z$, respectively, in Eqs. (8) and (9), to obtain the quantum transformations [19].

From the commutation relation

$$\left[\widehat{S}_x, \widehat{S}_y\right] = \mathrm{i}2\widehat{S}_z \tag{16}$$

and its cyclic permutations, it is clear that in the quantum world all the quantities corresponding to the Stokes operators cannot be well defined simultaneously, due to the Heisenberg uncertainty relation. As the variance of one Stokes operator can be made smaller if another is allowed to increase, the concept of "polarization squeezing" has been discussed [7,8,20–22].

4. Classical theory of our experiment

Let us now assume that we measure the intensity of the horizontal component of a state while varying a geometric rotation. Assume further that the detected intensity is found to be constant for all geometric rotations. Recall that the measured intensity corresponds to the projection onto the s_z-axis, and that the geometric rotations are equivalent to rotations around the s_y-axis. It is then easily seen that the only points on the Poincaré sphere that have a constant projection onto the s_z-axis for all geometric rotations are the north and south pole ($s_y = \pm 1$). Hence, the field must be circularly polarized.

Applying a relative phase shift of $\pi/2$ to the circularly polarized state would map it onto the equator of the Poincaré sphere. Subsequent geometric rotation would then move the state along the equator. Consequently, the projection onto the s_z-axis would then take all the values between -1 and $+1$. In other words, the detector would show full visibility as the rotation angle θ is varied. If we allow for stochastic (or quasi-monochromatic) fields, the average values of the different Stokes parameters characterize the state of the field. The corresponding points will then lie inside the Poincaré sphere. Since the states can be described by a probability distribution on the sphere, their averages obey the same transformation rules as the monochromatic fields, i.e., the transformations can be seen as rotations. This means that all the states represented by points on the s_y-axis will result in a constant intensity in the first measurement considered above. These states can be seen as circularly polarized fields of different degrees. Using the usual definition of the degree of polarization [3]

$$\eta = \sqrt{s_x^2 + s_y^2 + s_z^2} \tag{17}$$

and Eq. (11), it is seen that the visibility V in the second intensity measurement equals the degree of polarization

$$V = \frac{I_{\max} - I_{\min}}{I_{\max} + I_{\min}} = \eta. \tag{18}$$

5. Experimental realization and measurement results

In this section, we report on our experiment and relate our results to the classical theory. A fully quantum mechanical treatment of the experiment is presented in the following section.

The experiment described in the previous section was carried out on photon pairs generated by type-II spontaneous parametric down conversion. The theory of this process is well known [23–26] and it has allowed a wide range of experiments in fundamental quantum physics [10,27–29]. In our experiment, we used 1-ps pulses of wavelength 780 nm from a Ti:sapphire laser, which was pumped by an Ar-ion laser. The pulse repetition rate was 80 MHz and the pulses were frequency doubled before they entered a beta barium borate crystal of length 0.5 mm. Collinearly propagating 780-nm photon pairs, consisting of one

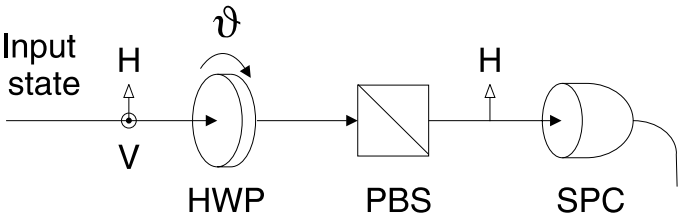

Fig. 3. The setup for the first measurement, corresponding to geometric rotation of the input state. Instead of spatial rotation of the source or the detector, a HWP was used. In the second measurement, the HWP was replaced by a quarter-wave plate. The intensity measurement of a horizontal linearly polarized component (H) was realized by using a polarization beam splitter (PBS) to spatially separate it from the vertical one (V).

horizontally polarized and one vertically polarized photon, were created in the crystal. The generated down-converted light was subsequently filtered spatially, by irises, and temporally, by preceding each of the detectors with a 10-nm passband optical filter. The linearly polarized modes could then easily be coupled by rotating phase plates that were placed in the beam. The photon-counting measurement was achieved using EG&G single-photon counters with a quantum efficiency of 65% for the wavelength used. However, in order to simplify the alignment, the light was guided to the detectors by fibers, which together with other losses made the overall detection efficiency about 5%.

In two related experiments [30,31] employing spontaneous parametric down conversion, transformations among three mutually orthogonal two-photon states were realized by simply rotating phase plates.

The setup for our first measurement is schematically shown in Fig. 3. Instead of physically rotating the detection part relative to the source, we rotated a half-wave plate (HWP). This can be seen as a phase shift of π in the rotated basis defined by the HWP. The total effect on the state in the original basis is therefore equivalent to a geometric rotation to the basis of the HWP followed by the phase shift and a second rotation back to the original basis. The resulting transformation matrix can be written

$$\begin{pmatrix} \cos\vartheta & -\sin\vartheta \\ \sin\vartheta & \cos\vartheta \end{pmatrix}\begin{pmatrix} 1 & 0 \\ 0 & \mathrm{e}^{-\mathrm{i}\pi} \end{pmatrix}\begin{pmatrix} \cos\vartheta & \sin\vartheta \\ -\sin\vartheta & \cos\vartheta \end{pmatrix} = \begin{pmatrix} \cos 2\vartheta & \sin 2\vartheta \\ \sin 2\vartheta & -\cos 2\vartheta \end{pmatrix}$$
$$= \begin{pmatrix} 1 & 0 \\ 0 & \mathrm{e}^{-\mathrm{i}\pi} \end{pmatrix}\begin{pmatrix} \cos 2\vartheta & \sin 2\vartheta \\ -\sin 2\vartheta & \cos 2\vartheta \end{pmatrix}. \tag{19}$$

Thus, rotation of a HWP by ϑ is equivalent to a geometric rotation of 2ϑ followed by a relative phase shift of π. In the Poincaré-sphere representation, this corresponds to rotating the sphere by 4ϑ around the s_y-axis and then turning it upside down.

As seen in Fig. 4, we obtained a constant intensity when the rotation angle ϑ was varied. The same reasoning and conclusion as above then applies: The only possible states that can give rise to these results are the ones on the s_y-axis (since turning the Poincaré sphere upside down maps the s_z-axis onto itself).

As described previously, these states would produce interference fringes with visibility of its degree of polarization when geometrically rotated after being phase shifted by $\pi/2$. In the second measurement, we therefore replaced the HWP with a quarter-wave plate. As in the case of the HWP, rotation of the quarter-wave plate could be seen as a geometric rotation followed by a relative phase shift and a geometric rotation back to the original basis. Now, since the considered states are located on the s_y-axis, the first rotation leaves the states unchanged. The relative phase shift of $\pi/2$ induced by the quarter-wave plate and the subsequent geometric rotation would then map the states onto the equatorial plane, rotating them around the s_y-axis with twice the rotation angle of the quarter-wave plate.

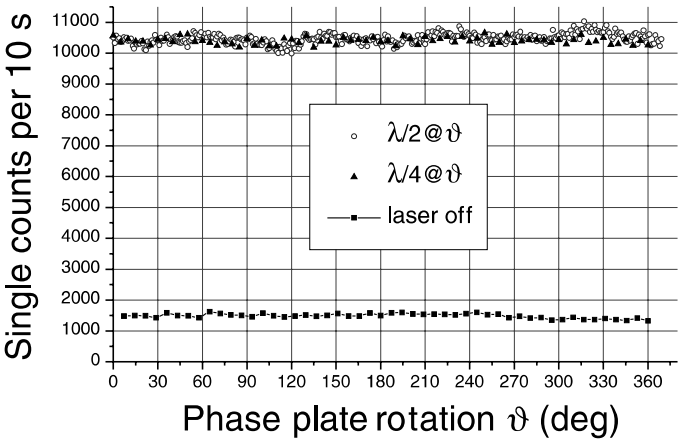

Fig. 4. The results of the first two measurements described in Fig. 3. Single counts per 10 s as a function of the rotation angle ϑ of the HWP (○) and the quarter-wave plate (▲). For comparison, the dark counts (■) measured when the laser was switched off are plotted.

The measured intensity as a function of the rotation angle of the quarter-wave plate is also plotted in Fig. 4. Again, the intensity is found to be constant, which implies no degree of polarization. That is, according to the classical theory, the light is unpolarized and the point characterizing the average values of the Stokes parameters lies in the center of the Poincaré sphere.

However, we also performed a third measurement, which is described in Fig. 5. The setup is the same as that used in our first measurement, but this time we measured the coincidences of detecting one photon in each of the two linear polarizations when rotating the HWP. This is a fourth-order correlation measurement, whereas the previous were second-order correlation measurements. As shown in Fig. 6, this allowed us to obtain interference fringes with a visibility attaining 76%. Let us now recall the accepted quantum optical definition of an unpolarized two-mode state [32–39]. Such a state must be invariant to any combination of geometric rotations and relative phase shifts. Our state is clearly not invariant to the combination of geometric rotations and relative phase shifts imparted by the HWP. Therefore, it is not unpolarized in the quantum theory. Thus, the considered state ($|1,1\rangle$) has quantum polarization properties that cannot be explained classically.

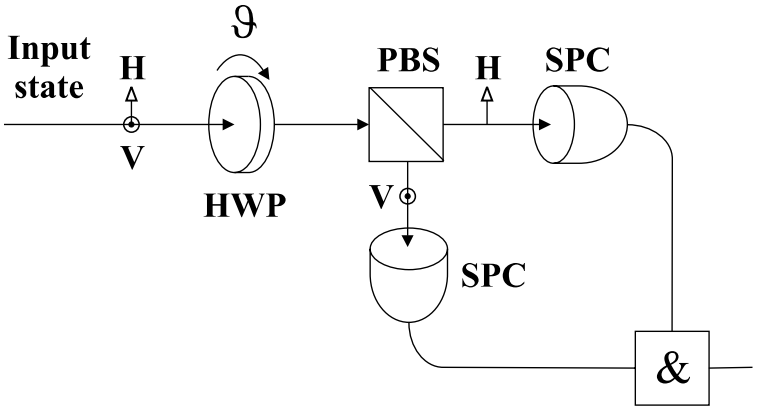

Fig. 5. The setup for the coincidence measurement.

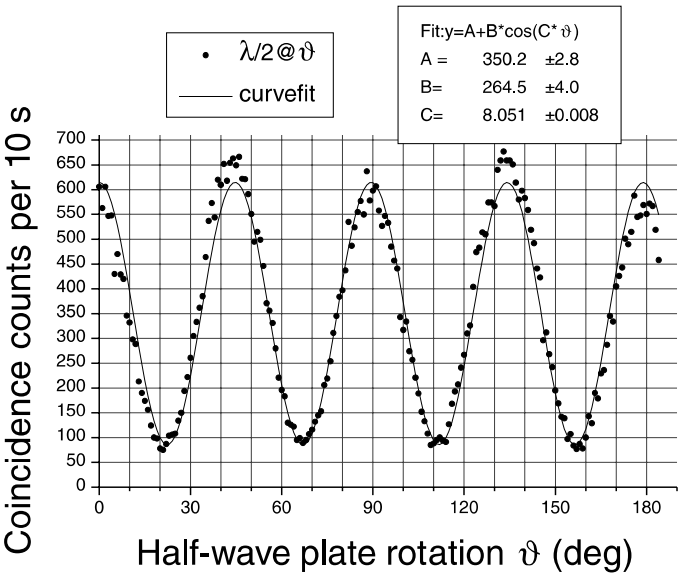

Fig. 6. The result of the measurement described in Fig. 5. The measured number of coincidence counts per 10 s (●) as a function of the rotation angle ϑ of the HWP. The curve fit shows a visibility of 76%.

6. Quantum theory of our experiment

We have seen that the classical theory cannot explain the outcomes of our measurements. In this section, we therefore give the quantum theory for the different measurements. We have chosen to keep the presentation rather detailed for pedagogical reasons. This should also make it easy to use the presented theory in related experiments. As we think it is, to this end, more transparent to transform the states than the operators, we here make use of the Schrödinger picture. We derive the transformations of the states in the second excitation manifold, i.e., for states with exactly two photons. Any such a (pure) normalized state can be written

$$|\Psi\rangle = c_0|0,2\rangle + c_1|1,1\rangle + c_2|2,0\rangle, \tag{20}$$

where c_0, c_1, $c_2 \in \mathbb{C}$, $|c_0|^2 + |c_1|^2 + |c_2|^2 = 1$, and $|m,n\rangle$ denotes the state with m (n) photons in the horizontally (vertically) polarized mode. The relative phase shift in Eq. (2) corresponds to the quantum transformation $\widehat{U}_{\mathrm{PS}}(\phi) = \exp(-\mathrm{i}\hat{b}^{\dagger}\hat{b}\phi)$. The state (20) is then transformed according to $\widehat{U}_{\mathrm{PS}}(\phi)\,|\Psi\rangle$, which can be expressed in matrix form as

$$\begin{pmatrix} c_0' \\ c_1' \\ c_2' \end{pmatrix} = \begin{pmatrix} \mathrm{e}^{-\mathrm{i}2\phi} & 0 & 0 \\ 0 & \mathrm{e}^{-\mathrm{i}\phi} & 0 \\ 0 & 0 & 1 \end{pmatrix} \begin{pmatrix} c_0 \\ c_1 \\ c_2 \end{pmatrix} = \mathbf{U}_{\mathrm{PS}}^{(2)}(\phi) \begin{pmatrix} c_0 \\ c_1 \\ c_2 \end{pmatrix}. \tag{21}$$

Similarly, the transformations corresponding to geometric rotations are found to be $\widehat{U}_{\mathrm{GR}}(\theta) = \exp(-\mathrm{i}\widehat{S}_y\theta)$, and the transformation matrix in the second manifold is

$$\mathbf{U}_{\mathrm{GR}}^{(2)}(\theta) = \begin{pmatrix} \cos^2\theta & -(1/\sqrt{2})\sin 2\theta & \sin^2\theta \\ (1/\sqrt{2})\sin 2\theta & \cos 2\theta & -(1/\sqrt{2})\sin 2\theta \\ \sin^2\theta & (1/\sqrt{2})\sin 2\theta & \cos^2\theta \end{pmatrix}. \tag{22}$$

This transformation also describes a lossless beam splitter, which couples two spatially modes.

A beam passing through a phase retarder rotated by ϑ (as defined in Figs. 3 and 5), results in the transformation $\widehat{U}_{\mathrm{GR}}(-\vartheta)\widehat{U}_{\mathrm{PS}}(\phi)\widehat{U}_{\mathrm{GR}}(\vartheta)$, where ϕ is the delay of the horizontal mode as $\vartheta = 0$. As described previously, this is realized by noting that the effect can be seen as a relative phase shift ϕ in the basis defined by the retarder.

It follows that the effects of the rotated HWP and quarter-wave plate in the second manifold are given by

$$\mathbf{U}^{(2)}_{\mathrm{HWP}}(\vartheta) = \mathbf{U}^{(2)}_{\mathrm{GR}}(-\vartheta)\cdot\mathbf{U}^{(2)}_{\mathrm{PS}}(\pi)\cdot\mathbf{U}^{(2)}_{\mathrm{GR}}(\vartheta) = \begin{pmatrix} \cos^2 2\vartheta & -(1/\sqrt{2})\sin 4\vartheta & \sin^2 2\vartheta \\ -(1/\sqrt{2})\sin 4\vartheta & -\cos 4\vartheta & (1/\sqrt{2})\sin 4\vartheta \\ \sin^2 2\vartheta & (1/\sqrt{2})\sin 4\vartheta & \cos^2 2\vartheta \end{pmatrix} \tag{23}$$

and

$$\begin{aligned}\mathbf{U}^{(2)}_{\mathrm{QWP}}(\vartheta) &= \mathbf{U}^{(2)}_{\mathrm{GR}}(-\vartheta)\cdot\mathbf{U}^{(2)}_{\mathrm{PS}}(\pi/2)\cdot\mathbf{U}^{(2)}_{\mathrm{GR}}(\vartheta) \\ &= \begin{pmatrix} (\sin^2\vartheta - \mathrm{i}\cos^2\vartheta)^2 & (1/\sqrt{2})(1-\mathrm{i}\cos 2\vartheta)\sin 2\vartheta & (\mathrm{i}/2)\sin^2 2\vartheta \\ (1/\sqrt{2})(1-\mathrm{i}\cos 2\vartheta)\sin 2\vartheta & -\mathrm{i}\cos^2 2\vartheta & (1/\sqrt{2})(1+\mathrm{i}\cos 2\vartheta)\sin 2\vartheta \\ (\mathrm{i}/2)\sin^2 2\vartheta & (1/\sqrt{2})(1+\mathrm{i}\cos 2\vartheta)\sin 2\vartheta & (\cos^2\vartheta - \mathrm{i}\sin^2\vartheta)^2 \end{pmatrix},\end{aligned} \tag{24}$$

respectively. Hence, the states that impinged on the detectors in our measurements are given by $\mathbf{U}^{(2)}_{\mathrm{HWP}}(\vartheta)(0,1,0)^{\mathrm{T}}$ and $\mathbf{U}^{(2)}_{\mathrm{QWP}}(\vartheta)(0,1,0)^{\mathrm{T}}$. Thus, when the HWP was used, the state was

$$|\Psi_{\mathrm{HWP}}(\vartheta)\rangle = -\frac{\sin 4\vartheta}{\sqrt{2}}|0,2\rangle - \cos 4\vartheta|1,1\rangle + \frac{\sin 4\vartheta}{\sqrt{2}}|2,0\rangle. \tag{25}$$

It follows that the average photon number in the horizontal mode was $\langle\Psi_{\mathrm{HWP}}(\vartheta)|\hat{a}^{\dagger}\hat{a}|\Psi_{\mathrm{HWP}}(\vartheta)\rangle = 1$, for any rotation angle ϑ. Similarly, in the case of the quarter-wave plate we had the state

$$|\Psi_{\mathrm{QWP}}(\vartheta)\rangle = \frac{(1-\mathrm{i}\cos 2\vartheta)\sin 2\vartheta}{\sqrt{2}}|0,2\rangle - \mathrm{i}\cos^2 2\vartheta|1,1\rangle + \frac{(1+\mathrm{i}\cos 2\vartheta)\sin 2\vartheta}{\sqrt{2}}|2,0\rangle, \tag{26}$$

which means that the average photon number impinging on the detector was $\langle\Psi_{\mathrm{QWP}}(\vartheta)|\hat{a}^{\dagger}\hat{a}|\Psi_{\mathrm{QWP}}(\vartheta)\rangle = 1$. Unfortunately, our detectors are far from 100% efficient and do not register all the impinging photons. It is readily shown that as long as the detectors are linear, albeit not 100% efficient, the detected count rate is still independent of ϑ. However, the detectors being avalanche photodiodes, they are not linear, and in general absorption of either one or two photons generates only one avalanche burst. Taking this effect into account, one finds in fact that the count rate should not be independent of ϑ. For low quantum efficiencies this effect is small, however, and at the present detection quantum efficiency of 5%, the visibility of the expected ensuing curve would be only 1%. This is well below the count rate noise, which essentially follow a Poissonian distribution. This explains the apparently invariant number of counts under geometric rotation in the first two measurements.

In the third measurement, we detected one photon in each polarization simultaneously. In theory, the probability for this outcome is

$$|\langle 1,1|\Psi_{\mathrm{HWP}}(\vartheta)\rangle|^2 = \frac{1+\cos 8\vartheta}{2}. \tag{27}$$

Of course, we did not get coincidence counts with probability one for any angle, since the detectors' quantum efficiency was far from perfect. However, our measurements were proportional to the theoretical prediction, apart from a bias due to dark counts, as expected.

It is now also seen theoretically that the state $|1,1\rangle$ has quantum polarization properties. From the classical theory, $|1,1\rangle$ was previously seen to be unpolarized. This could perhaps be expected since the fields of the two perpendicular polarization modes are equally excited and phase invariant.

We note that the classical requirements for an unpolarized state can be expressed as conditions on second-order correlation functions only. This is in contrast to quantum theory, which, as noted by Agarwal [32], sets conditions on higher-order correlation functions too. Apart from the two-mode vacuum state, the unpolarized quantum states are found to be mixed states [32–39]. It should be noted that we here deal with strictly two-mode transverse fields, that is, we implicitly assume that the field can be described by a single temporal mode, since the two (geometrical) transverse modes exhaust the considered set of modes. Therefore, the temporal invariance of the Verdet–Stokes conditions discussed in the context of unpolarized fields by Barakat [4] does not apply.

As seen in Eq. (27), the theory predicts that the coincidence measurement would give full visibility. This fact was pointed out by Klyshko [7], who noted that the states $|n,n\rangle$ are unpolarized in the classical (second-order) sense but completely polarized in the fourth order.

A somewhat related experiment was reported in Ref. [40]. There two collinearly propagating, correlated laser beams of perpendicular linear polarization and with same intensity were used. As they were rotated, the noise of their intensity difference was measured. The noise was shown to vary sinusoidally as a function of the rotation angle, and to attain values below the standard quantum limit for given angles. As explained in Ref. [41], this could be seen as quantum polarization properties of a classically unpolarized light. However, the wavelengths of the two beams were different, and therefore the experiment must be described using four modes.

7. Quantum treatment of polarization

In the classical theory of polarization, all the linearly polarized states can be transformed into each other by geometric rotations. Since the ratio between the horizontal and vertical component fully characterizes any linearly polarized field, they can in theory be distinguished by one single measurement (on a single "pulse" of light, for example). In reality, though, the measurements will be deteriorated due to shot noise.

In quantum optics too, the linearly polarized states can be mapped onto each other by geometric rotations. Similarly, the ratio between the expectation values of the horizontal and vertical components will be unique for every such state. However, in general these states will not be orthogonal, and therefore they cannot be distinguished by one single measurement due to the probabilistic nature of quantum mechanics. In particular, let us consider a linearly polarized state with N photons in the horizontal mode. Any other linearly polarized N-photon state can then be generated by geometrical rotating the original state $|N,0\rangle$ by a given angle. Their overlap is found to be

$$\left|\langle N,0|\mathrm{e}^{-\mathrm{i}\hat{S}_y\theta}|N,0\rangle\right|^2 = (\cos\theta)^{2N}, \tag{28}$$

which shows that they are orthogonal if and only if $\theta = \pm\pi/2$. Note that all the pure linearly polarized states can be written

$$\sum_{N=0}^{\infty} a_N \mathrm{e}^{-\mathrm{i}\hat{S}_y\theta}|N,0\rangle, \quad a_N \in \mathbb{C}, \ \ |a_0| < 1, \tag{29}$$

where we have assumed the states to be normalized, and considered the vacuum state ($|a_0|^2 = 1$) to be unpolarized. Any state of the form (29) will pass through a perfect polarizer oriented at the angle θ without loss. These states are in general entangled. However if, e.g., the horizontal mode of the unrotated field is in

the coherent state $|\alpha\rangle$, we have $a_N = \alpha^N \exp(-|\alpha|^2/2)/\sqrt{N!}$, and the horizontal and the vertical mode of the rotated state will be in a product state of two coherent states.

We see from Eq. (28) that the states $|N,0\rangle$ cannot form a complete set in excitation manifolds $N > 1$ by applying geometric rotations. This means that using these states, we cannot perfectly distinguish different rotation angles if $N > 1$. In such a case, we would like to construct a measurement corresponding to a complementary observable to the generator of the rotation, i.e., a Hermitian operator whose eigenstates are superpositions of all the eigenstates of the generator equally weighted.

The eigenstates of the considered generator $\widehat{S}_y$ are invariant under geometric rotation. Among these, we find the classical circularly polarized and unpolarized light. We denote the $N+1$ orthogonal N-photon eigenstates as $|\mathrm{o}_k^{(N)}\rangle$, $k = 0,1,\ldots,N$. Using the notation $|m,n\rangle_{\mathrm{o}}$ for the state with m (n) photons in the left-hand (right-hand) circularly polarized mode, we can write $|\mathrm{o}_k^{(N)}\rangle = |N-k,k\rangle_{\mathrm{o}}$. That is, the eigenstates of $\widehat{S}_y$ are the circularly polarized two-mode number states. Constructing an equipartition state of these as described above

$$|\zeta^{(N)}\rangle = \frac{1}{\sqrt{N+1}} \sum_{k=0}^{N} \mathrm{e}^{\mathrm{i}\phi_k^{(N)}} |\mathrm{o}_k^{(N)}\rangle, \quad \phi_k^{(N)} \in \mathbb{R}, \tag{30}$$

we find

$$\left| \langle \zeta^{(N)} | \mathrm{e}^{-\mathrm{i}\hat{S}_y\theta} | \zeta^{(N)} \rangle \right|^2 = \frac{\sin^2([N+1]\theta)}{(N+1)^2 \sin^2\theta}. \tag{31}$$

Thus, employing the states (30), the rotation angles $\theta_k^{(N)} = \pi k/(N+1)$, $k = 0,1,\ldots,N$, can be distinguished perfectly, since they are mutually orthogonal. Hence, the Hermitian rotation-angle operator can be written

$$\widehat{\Theta} = \sum_{N=0}^{\infty} \sum_{k=0}^{N} \theta_k^{(N)} |\zeta_k^{(N)}\rangle\langle\zeta_k^{(N)}|, \tag{32}$$

where

$$|\zeta_k^{(N)}\rangle = \mathrm{e}^{-\mathrm{i}\hat{S}_y\theta_k^{(N)}} |\zeta^{(N)}\rangle. \tag{33}$$

We stress that the eigenstates of the rotation-angle operator are not linearly polarized, which could be expected from an analogy with classical optics. Note also that $|\zeta_0^{(0)}\rangle = |0,0\rangle$ was included in Eq. (32) to make the set of projectors complete. The corresponding outcome, of course, does not give any information of the angle of rotation, since $|\zeta_0^{(0)}\rangle = |\mathrm{o}_0^{(0)}\rangle$ is an eigenstate of $\widehat{S}_y$ and therefore invariant under geometric rotations. Hence, the value of $\theta_0^{(0)}$ has no significance and it can be chosen arbitrarily.

For given choices of equipartition states (30) in the different manifolds N, we can introduce the corresponding probability distribution functions. For a state described by the density operator $\hat{\rho}$, they take the form

$$P_{\hat{\rho}}^{(N)}(\theta) = \langle \zeta^{(N)} | \mathrm{e}^{\mathrm{i}\hat{S}_y\theta} \hat{\rho}\, \mathrm{e}^{-\mathrm{i}\hat{S}_y\theta} | \zeta^{(N)} \rangle. \tag{34}$$

These functions are π-periodic and satisfy

$$\sum_{N=0}^{\infty} \sum_{k=0}^{N} P_{\hat{\rho}}^{(N)}(\theta_k^{(N)}) = 1. \tag{35}$$

For more properties of these functions, see the corresponding discussion in the context of relative phase [12]. Recently, a two-photon rotation-angle eigenstate was realized and its probability distribution function measured [31].

8. Summary

We have performed a rather simple two-photon experiment, which allowed us to verify differences between the classical and the quantum theory of polarization. Only for states containing at most one photon are the theories fully compatible. The reason is that in a proper quantum theory, higher than second-order correlations in the field amplitudes are incorporated in the theory, whereas in the classical description of two-mode fields such correlations follow from the Stokes parameters, since the relative properties of the field modes are then fully characterized by three real numbers. Therefore, absence of second-order correlations, e.g., will lead to absence of higher-order correlations for classical fields, whereas our experiment shows that this is not necessarily the case for quantized fields.

In our experiment, we used pulses of photon pairs generated by spontaneous parametric down conversion of type II. The experiment consisted of three measurements, whose (classical) effects were easily described using a geometrical representation of the Stokes parameters. The first two measurements were seen to imply that the considered state was unpolarized by the classical theory. Despite this, our third measurement was found to depend on the rotation angle around the direction of propagation. The quantum theory explaining our results was given and a way of treating polarization in quantum optics was outlined.

Acknowledgements

This work was supported by the Swedish Institute, the Royal Swedish Academy of Science (KVA), the Swedish Research Council for Engineering Sciences (TFR), the Swedish Foundation for Strategic Research (SSF), and the Swedish Natural Science Research Council (NFR).

References

[1] G.G. Stokes, Trans. Cambridge Philos. Soc. 9 (1852) 399; W. Swindell (Ed.), Polarized Light, Dowden, Stroudsburg, 1975, p. 124 (reprint).
[2] E. Hecht, Am. J. Phys. 38 (1970) 1156–1158.
[3] M. Born, E. Wolf, Principles of Optics, Pergamon, London, 1959.
[4] R. Barakat, J. Opt. Soc. Am. A 6 (1989) 649–659.
[5] A. Luis, L.L. Sánchez-Soto, Prog. Opt. 41 (2000) 421.
[6] D.N. Klyshko, Phys. Lett. A 163 (1992) 349–355.
[7] D.M. Klyshko, Sov. Phys. JETP 84 (1997) 1065–1079.
[8] A.P. Alodjants, S.M. Arakelian, A.S. Chirkin, Quant. Semiclass. Opt. 9 (1997) 311–329.
[9] M.Ya. Agre, Opt. Spectrosc. 89 (2000) 445–452.
[10] P. Hariharan, B.C. Sanders, Prog. Opt. 36 (1996) 49–128.
[11] A. Luis, L.L. Sánchez-Soto, Phys. Rev. A 48 (1993) 4702–4708.
[12] G. Björk, J. Söderholm, J. Opt. B 1 (1999) 315–319.
[13] A. Trifonov, T. Tsegaye, G. Björk, J. Söderholm, E. Goobar, M. Atatüre, A.V. Sergienko, J. Opt. B 2 (2000) 105–112.
[14] V.P. Karassiov, V.L. Derbov, S.I. Vinitsky, Proc. SPIE 2098 (1994) 164–171.
[15] U. Fano, J. Opt. Soc. Am. 39 (1949) 859–863.
[16] J.M. Jauch, F. Rohrlich, The Theory of Photons and Electrons, Addison-Wesley, Cambridge, 1955.
[17] E. Collett, Am. J. Phys. 38 (1970) 563–574.
[18] J. Schwinger, On Angular Momentum, US Atomic Energy Commission Report No. NYO-3071, 1952 (unpublished); L.C. Biedenharn, H. van Dam (Eds.), Quantum Theory of Angular Momentum, Academic, New York, 1965, p. 229 (reprint).
[19] B. Yurke, S.L. McCall, J.R. Klauder, Phys. Rev. A 33 (1986) 4033–4054.
[20] R. Tanaś, S. Kielich, J. Mod. Opt. 37 (1990) 1935–1945.
[21] R. Tanaś, Ts. Gantsog, J. Mod. Opt. 39 (1992) 749–760.
[22] A.S. Chirkin, A.A. Orlov, D.Yu. Parashchuk, Sov. J. Quant. Electron. 23 (1993) 870–874.
[23] W.H. Louisell, A. Yariv, A.E. Siegman, Phys. Rev. 124 (1961) 1646–1654.

[24] C.K. Hong, L. Mandel, Phys. Rev. A 31 (1985) 2409–2418.
[25] M.H. Rubin, D.N. Klyshko, Y.H. Shih, A.V. Sergienko, Phys. Rev. A 50 (1994) 5122–5133.
[26] T.E. Keller, M.H. Rubin, Phys. Rev. A 56 (1997) 1534–1541.
[27] D.C. Burnham, D.L. Weinberg, Phys. Rev. Lett. 25 (1970) 84–87.
[28] P.G. Kwiat, K. Mattle, H. Weinfurter, A. Zeilinger, Phys. Rev. Lett. 75 (1995) 4337–4341.
[29] A. Zeilinger, Rev. Mod. Phys. 71 (1999) S288–S297.
[30] A.V. Burlakov, M.V. Chekhova, O.A. Karabutova, D.N. Klyshko, S.P. Kulik, Phys. Rev. A 60 (1999) R4209–R4212.
[31] T. Tsegaye, J. Söderholm, M. Atatüre, A. Trifonov, G. Björk, A.V. Sergienko, B.E.A. Saleh, M.C. Teich, Phys. Rev. Lett. 85 (2000) 5013–5017.
[32] G.S. Agarwal, Lett. Nuovo Cimento 1 (1971) 53–56.
[33] H. Prakash, N. Chandra, Phys. Lett. A 34 (1971) 28–29.
[34] H. Prakash, N. Chandra, Phys. Rev. A 4 (1971) 796–799.
[35] H. Prakash, N. Chandra, Phys. Rev. A 9 (1974) 1021.
[36] C.L. Mehta, M.K. Sharma, Phys. Rev. D 10 (1974) 2396–2398.
[37] J. Lehner, U. Leonhardt, H. Paul, Phys. Rev. A 53 (1996) 2727–2735.
[38] G.S. Agarwal, J. Lehner, H. Paul, Opt. Commun. 129 (1996) 369–372.
[39] J. Söderholm, G. Björk, A. Trifonov, quant-ph/0007099.
[40] A. Heidmann, R.J. Horowicz, S. Reynaud, E. Giacobino, C. Fabre, G. Camy, Phys. Rev. Lett. 59 (1987) 2555–2557.
[41] V.P. Karasev, A.V. Masalov, Opt. Spectrosc. 74 (1993) 551–555.